



Letters

A Novel Miniaturized Polarization Independent Band-Stop Frequency Selective Surface

Sayi Soundariya Sampath , Ramprabhu Sivasamy , and K. J. Jegadish Kumar

Abstract—A novel miniaturized frequency selective surface (FSS) with a band-stop response at 1.6 GHz is presented in this letter. The designed FSS comprises convoluted elements connected via plated-through holes, which increases the overall electrical length. The proposed FSS unit cell provides the miniaturization of $0.034 \lambda_0 \times 0.034 \lambda_0$, where λ_0 is the free space wavelength corresponding to the resonant frequency. The drafted FSS is polarization independent and angularly stable for both TE and TM polarizations. A prototype of the FSS is fabricated and its simulated results are validated with measurements.

Index Terms—Frequency selective surface (FSS), plated-through holes (PTH), radio-frequency interference (RFI).

I. INTRODUCTION

FREQUENCY selective surface (FSS) is a structure consisting of two or three-dimensional periodic elements, which exhibits frequency filtering properties [1]–[4]. The periodic array of slots in a perfectly conducting sheet acts as a bandpass filter, passing waves at the resonant frequency of the slots but rejecting them at higher and lower frequencies. On the contrary, the array of conducting patches acts as a band-stop filter, rejecting waves at the patch's resonant frequency but passing them at higher and lower frequencies [5]. Of late FSSs with miniaturized unit cell designs are widely discussed owing to its space constraint applications and enhanced performances. Plenty of techniques are discussed in the literature regarding the miniaturization of the FSS unit cell. A dual-band FSS with closely spaced resonance has achieved a miniaturization of $0.065 \lambda_0 \times 0.065 \lambda_0$ that cannot be considered as small scale [6]. In [7], novel ultrathin dual-band FSS used for X-band applications by controlling the current path along the vertical, horizontal, and rotational arm is illustrated. An anchor-shaped loop structure with dual-band-stop response is used to shield 2.4 and 5.0 GHz to protect the WLAN signal from being interfered. Tuning of the resonance frequency by adjusting the gap between two adjacent

anchor-loaded loops is possible only to an extent, beyond which the loops tend to overlap [8]. A dual-band FSS with crooked cross geometry works as a shielding component for the S-band operations is also discussed [9]. Crossed dipoles in the form of swastika achieve the smallest dimension of the unit cell is portrayed in [10]. A low-profile paper substrate-based FSS for shielding the GSM applications is discussed in [11], where the unit cell is evolved by convoluting the inner square loop and adding stubs to the outer square loop element. Wireless charging pads generate radio-frequency interference (RFI) that can degrade the signal transmission and reception of portable communication devices, therefore, the use of an FSS is proposed for reducing the RFI [12]. The physical footprint of the FSS discussed in [12] is complex in nature. FSS exhibits wide tuning of band-stop response and provides electromagnetic (EM) shielding in different bands. Wideband tunable FSS structure with an embedded biasing network exhibits broadband attenuation of 1.28 GHz [13]. Reconfigurable FSS with a pair of shorted square loops have been proposed for EM shielding applications. Varying the spacing between square loops satisfies frequency reconfiguration, but tends to deteriorate the property of miniaturization [14]. Hence, there is a need for an FSS with miniaturized unit cell geometry along with polarization and angular independent operation.

In this letter, a novel miniaturized FSS with band-stop characteristics is proposed. The FSS has the overall size of $0.034 \lambda_0 \times 0.034 \lambda_0$ and also provides angular independent operation along with polarization independency.

Section II details the unit cell geometry of the proposed FSS. Section III provides the evolution of the FSS unit cell. In Section IV, simulated results for various modes with different incident angles are discussed. Parametric study of the proposed FSS is also explained in detail. Section V deals with the measurement setup used for the analysis.

II. UNIT CELL DESIGN

The top and bottom view of the proposed FSS unit cell geometry is shown in Fig. 1. The substrate used is FR4 (lossy) of thickness 1.6 mm with relative permittivity $\epsilon_r = 4.3$ having a loss tangent value of 0.025. The proposed FSS contains modified zigzag inductive arms on one side of the substrate and the same pattern with a small center portion being etched, is printed

Manuscript received March 10, 2018; revised April 20, 2018, May 31, 2018, and August 10, 2018; accepted August 27, 2018. Date of publication October 1, 2018; date of current version September 30, 2019. (Corresponding author: Sayi Soundariya Sampath.)

The authors are with the Department of Electronics and Communication Engineering, Sri Sivasubramaniya Nadar College of Engineering, Chennai 603110, India (e-mail: sayisoundariya@gmail.com; ramprabhus@ssn.edu.in; jegadishkj@ssn.edu.in).

Color versions of one or more of the figures in this letter are available online at <http://ieeexplore.ieee.org>.

Digital Object Identifier 10.1109/TEM.2018.2869664

0018-9375 © 2018 IEEE. Personal use is permitted, but republication/redistribution requires IEEE permission. See http://www.ieee.org/publications_standards/publications/rights/index.html for more information.

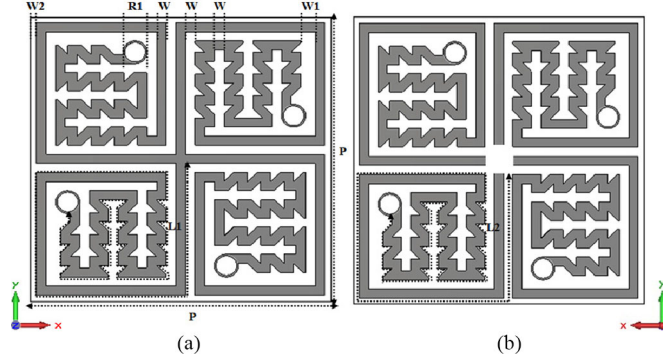


Fig. 1. (a) Top view of the FSS unit cell with dimensions $w = 0.2$ mm, $w1 = 0.3$ mm, $w2 = 0.15$ mm, $R1 = 0.5$ mm, $L1 = 24.725$ mm, and $P = 6.29$ mm. (b) Bottom view of the FSS unit cell with dimensions $L2 = 24.525$ mm.

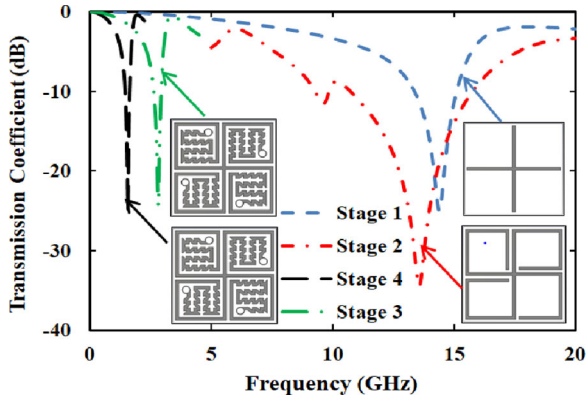


Fig. 2. Evolution of the proposed FSS.

on the other side of the substrate. The top and bottom layers are connected via plated-through holes (PTH). Incorporating 35 microns of copper plated PTH drills ($R1 = 0.5$ mm) provides proper continuity between the top and bottom layers. The purpose of the PTH drills is to increase the overall electrical length of the proposed FSS by extending the resonant path beneath its top layer. The dimensions of the FSS design are $w = 0.2$ mm, $w1 = 0.3$ mm, $w2 = 0.15$ mm, $R1 = 0.5$ mm, $P = 6.29$ mm, $L1 = 24.725$ mm, and $L2 = 24.525$ mm. Hence, the unit cell size of the proposed FSS is 6.29×6.29 mm².

III. EVOLUTION OF THE FSS UNIT CELL

The evolution of the proposed FSS and its simulated transmission characteristics for various stages are illustrated in Fig. 2. It is apparent that stage 1 begins with a simple crossed dipole design that resonates at 14.4 GHz. Stage 2 is obtained by convoluting the resonant arms that resonates at 13.5 GHz. Further shift in the resonant frequency is obtained by increasing the electrical length as in stage 3. It provides band-stop response at 2.8 GHz for the single layered FSS. Stage 4 comprises double-layered FSS, in which the electrical length of the top layer is extended by connecting it to the bottom layer via conductive holes. Increase in the electrical length shifts the resonance from 2.8 to 1.6 GHz. The proposed FSS with convoluted arms on both sides of the substrate with conductive holes helps in increasing its electrical length, hence, achieving miniaturization.

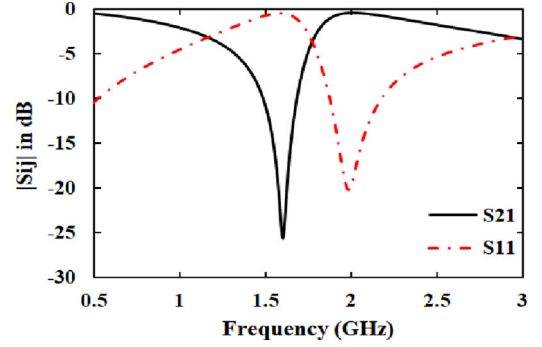


Fig. 3. Simulated S parameters of the proposed FSS.

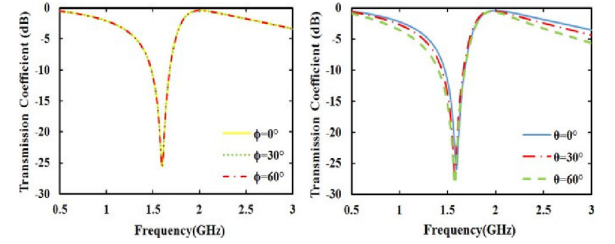


Fig. 4. Transmission coefficient of the proposed FSS for various angles of ϕ and θ in TE mode.

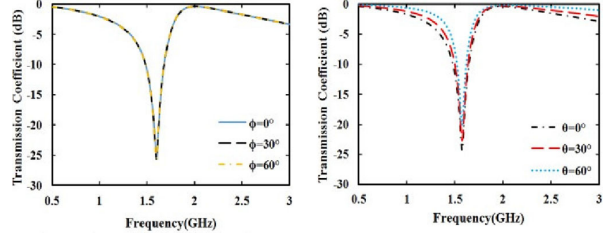


Fig. 5. Transmission coefficient of the proposed FSS for various angles of ϕ and θ in TM mode.

IV. SIMULATED RESULTS

The proposed FSS is simulated by using commercially available CST microwave studio. The floquet ports are used to study the performance of the proposed FSS. Periodic boundary conditions are assigned to the X and Y axes and the ports are placed along the Z -axis. Frequency domain solver is used to simulate the proposed FSS [11]. The simulated S parameters of the proposed FSS are shown in Fig. 3. The proposed FSS with its conductive patch elements acts as the band-stop filter for incident EM waves [5] at its operating frequency, which is defined by its convoluted structure. The convoluted FSS unit cell with its increased electrical length exhibits band-stop characteristics at 1.6 GHz with 26 dB attenuation.

Fig. 4 shows the simulated transmission characteristics of the proposed FSS for TE polarized EM fields at various angular incidences up to 60° for ϕ and θ . Similarly, Fig. 5 shows the simulated transmission characteristics of the proposed FSS for TM polarized EM fields at various angular incidences up to 60° for ϕ and θ [11], [13]–[15]. It is apparent that the proposed FSS offers stable response for any angle of incidence of the EM wave for any polarization at its resonant frequency of 1.6 GHz. Hence, the FSS satisfies angular independent and

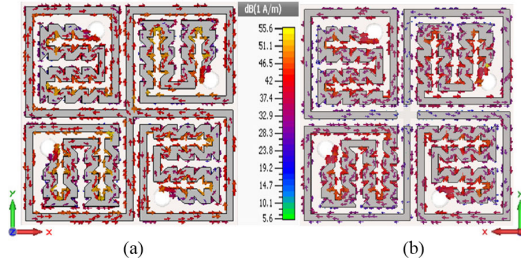


Fig. 6. Surface current distribution of the proposed FSS. (a) Top view. (b) Bottom view.

TABLE I
PARAMETRIC SWEEP

Parameters	Dimensions	Resonant frequency
Line width (w)	0.2 mm	1.6 GHz
Line width (w)	0.3 mm	1.96 GHz
Line width (w)	0.4 mm	2.32 GHz
Substrate thickness (h)	1.6 mm	1.6 GHz
Substrate thickness (h)	1.2 mm	1.67 GHz
Substrate thickness (h)	0.8 mm	1.79 GHz
Electrical length (L)	24.525 mm	1.6 GHz
Electrical length (L)	21.826 mm	1.76 GHz
Electrical length (L)	20.576 mm	1.95 GHz

polarization independent criteria enabling it to be a potential candidate for reflecting L -band signals at 1.6 GHz.

Surface current distribution of the proposed FSS is illustrated in Fig. 6. Resonant arms with high-surface current density are denoted by red color and those with low-surface current density are denoted by blue color.

A study on the influence of various design parameters on the resonant frequency of the FSS is presented in Table I. It is apparent that increase in the line width (w) from 0.2 to 0.4 mm shifts the resonant frequency from 1.6 to 2.32 GHz. Similarly decrease in the substrate thickness (h) from 1.6 to 0.8 mm shifts the resonant frequency from 1.6 to 1.79 GHz. In addition, decrease in the electrical length (L) from 24.525 to 20.576 mm shifts the resonant frequency from 1.6 to 1.95 GHz. The optimal parametric values of $w = 0.2$ mm, $h = 1.6$ mm, and $L = 24.525$ mm are chosen for designing the miniaturized, low-profile FSS to operate in the desired frequency of 1.6 GHz.

The terminating edge of the bottom layer can be increased or decreased in its length in order to change its resonant frequency. Here, the decrease in the electrical length increases the resonant frequency. This optimization is clearly depicted in Fig. 7.

V. MEASURED RESULTS

A. Normal Incidence

The measurement setup of the proposed FSS is shown in Fig. 8. A prototype of the FSS has been fabricated and is illustrated in Fig. 9. The overall dimension of the fabricated prototype measures 25.16 cm \times 25.16 cm that consists of 40 \times 40 elements spaced at 0.3 mm. The fabricated FSS is placed in a fixture surrounded by the absorbers and the corresponding

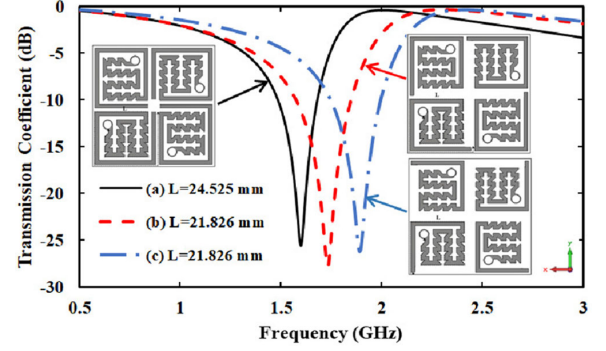


Fig. 7. Transmission coefficient of the proposed FSS for various of L . (a) $L = 24.525$ mm. (b) $L = 21.826$ mm. (c) $L = 20.576$ mm.

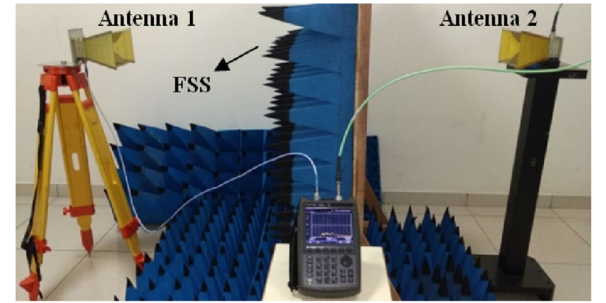


Fig. 8. Measurement setup with the fabricated prototype of the proposed FSS.

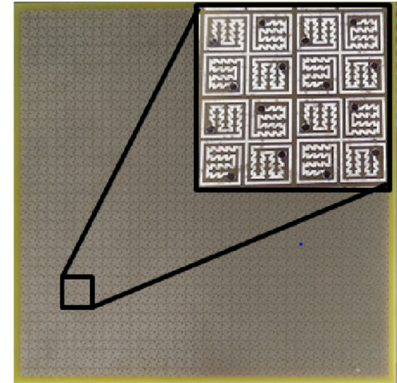


Fig. 9. Fabricated prototype of the proposed FSS.

results are recorded. Transmitting and receiving broadband horn antennas (JR12) with operating frequency of 1 to 12 GHz from verdant telemetry are used in the measurements. Initially the transmission characteristic is measured using a hand-held portable microwave analyzer from Agilent technologies (N9917A) without the FSS. Then, the fabricated FSS is placed in between the horn antennas and the transmission characteristics are recorded, which is normalized to obtain the measured result.

B. Oblique Incidence

Fig. 10 illustrates the comparison of the measured results at different incident angles with the simulated results [16]–[18]. It is observed that the proposed FSS offers stable response for an incident wave up to 60°. The measured results are TE polarized. It is evident that the measured results are in agreement with the simulated results. The measurement shows that the FSS

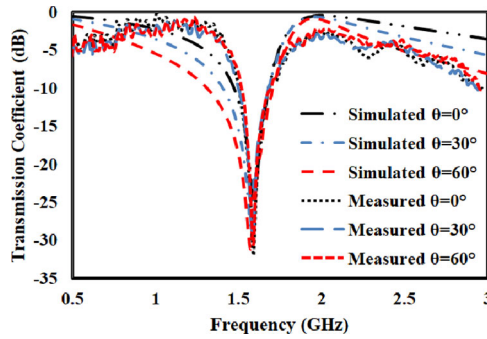


Fig. 10. Comparison of the measured and simulated results.

TABLE II
COMPARISON OF THE PROPOSED FSS WITH THE FSSs EXISTING
IN THE LITERATURE

Ref.	Resonant frequency	FSS unit cell size	Substrate	Miniaturization Technique
[6]	2.35, 3.05 GHz	$0.065 \lambda_0 \times 0.065 \lambda_0$	FR-4	Meandering
[7]	8.47, 10.45 GHz	$0.248 \lambda_0 \times 0.248 \lambda_0$	Arlon Di 880	L-shaped arms
[8]	2.4, 5 GHz	$0.065 \lambda_0 \times 0.076 \lambda_0$	F4B-2	Interlace grids
[9]	2.54, 3.54 GHz	$0.088 \lambda_0 \times 0.088 \lambda_0$	FR-4	Convoluted the arms
[10]	5 GHz	$0.116 \lambda_0 \times 0.116 \lambda_0$	FR-4	Crossed dipoles
[11]	930, 1720 MHz	$0.142 \lambda_0 \times 0.142 \lambda_0$	Paper	Modified square loop
[19]	3.28, 4.2, 5.4 GHz	$0.066 \lambda_0 \times 0.066 \lambda_0$	F4B-2	Convoluted the arms
This Work	1.6 GHz	$0.034 \lambda_0 \times 0.034 \lambda_0$	FR-4	Convoluted elements linked via PTH drills.

provides band-stop response at 1.6 GHz with 32 dB of attenuation at 0° of incident wave. The use of microwave absorbers reduced the edge effects and contributed to the peak value at its operating frequency [8], [13], [14], [19]. As the proposed FSS exhibits polarization independency due to its symmetrical geometry, the measured results for TE polarization holds good for TM polarization as well.

Table II compares the proposed miniaturized FSS with the FSSs available in the literature. The proposed FSS with single metal layer achieves miniaturization of $0.058 \lambda_0 \times 0.058 \lambda_0$ and the one with double metal layer achieves miniaturization of $0.034 \lambda_0 \times 0.034 \lambda_0$. Hence, the proposed FSS with single metal later exhibits better performance when compared to the existing FSSs and further miniaturization is achieved by the double layered structure. It is evident from the table that the proposed FSS with its convoluted geometry is compact and is a potential candidate for space constraint applications. Miniaturized FSSs are used in various applications including antenna reflectors, hybrid radomes, optical filters, and EM shields [20].

VI. CONCLUSION

Miniaturized band-stop FSS for reflecting L-band applications at 1.6 GHz is proposed in this letter. The FSS unit cell achieves miniaturization of $0.034 \lambda_0 \times 0.034 \lambda_0$. The proposed

design exhibits stable transmission performance at oblique incidences up to 60° . In addition, it satisfies polarization independent criteria.

REFERENCES

- [1] S. N. Azemi, K. Ghorbani, and W. S. T. Rowe, "3D frequency selective surface with incident angle independence," in *Proc. Eur. Microw. Conf.*, Nuremberg, Germany, 2013, pp. 928–931.
- [2] M. H. Nisanci *et al.*, "Experimental validation of a 3D FSS designed by periodic conductive fibers part-1: Band-pass filter characteristic," *IEEE Trans. Electromagn. Compat.*, vol. 59, no. 6, pp. 1841–1847, Dec. 2017.
- [3] M. H. Nisanci *et al.*, "Experimental validation of a 3D FSS designed by periodic conductive fibers part-2: Band-stop filter characteristic," *IEEE Trans. Electromagn. Compat.*, vol. 59, no. 6, pp. 1835–1840, Dec. 2017.
- [4] M. Bouslama, M. Traii, A. Gharsallah, and T. A. Denidni, "Reconfigurable dual-band 3D frequency selective surface unit-cell," in *Proc. IEEE Int. Symp. Antennas Propag. USNC/URSI Nat. Radio Sci. Meeting*, Vancouver, BC, Canada, 2015, pp. 1264–1265.
- [5] B. A. Munk, *Frequency Selective Surfaces: Theory and Design*, 1st ed. New York, NY, USA: Wiley, 2000.
- [6] S. Ghosh and K. V. Srivastava, "An angularly stable dual-band FSS with closely spaced resonances using miniaturized unit cell," *IEEE Microw. Wireless Compon. Lett.*, vol. 27, no. 3, pp. 218–220, Mar. 2017.
- [7] S. Ünalı, S. Çimen, G. Çakır, and U. E. Ayten, "A novel dual-band ultrathin FSS with closely settled frequency response," *IEEE Antennas Wireless Propag. Lett.*, vol. 16, pp. 1381–1384, 2017.
- [8] M. Yan *et al.*, "A miniaturized dual-band FSS with stable resonance frequencies of 2.4 GHz/5 GHz for WLAN applications," *IEEE Antennas Wireless Propag. Lett.*, vol. 13, pp. 895–898, 2014.
- [9] R. Sivasamy and M. Kanagasabai, "A novel dual-band angular independent FSS with closely spaced frequency response," *IEEE Microw. Wireless Compon. Lett.*, vol. 25, no. 5, pp. 298–300, May 2015.
- [10] R. Natarajan, M. Kanagasabai, S. Baisakhiya, R. Sivasamy, S. Palaniswamy, and J. K. Pakkathillam, "A compact frequency selective surface with stable response for WLAN applications," *IEEE Antennas Wireless Propag. Lett.*, vol. 12, pp. 718–720, 2013.
- [11] R. Sivasamy, L. Murugasamy, M. Kanagasabai, E. F. Sundarsingh, and M. Gulam Nabi Alsath, "A low-profile paper substrate-based dual-band FSS for GSM shielding," *IEEE Trans. Electromagn. Compat.*, vol. 58, no. 2, pp. 611–614, Apr. 2016.
- [12] P. Wu, F. Bai, Q. Xue, X. Liu, and S. Y. R. Hui, "Use of frequency-selective surface for suppressing radio-frequency interference from wireless charging pads," *IEEE Trans. Ind. Electron.*, vol. 61, no. 8, pp. 3969–3977, Aug. 2014.
- [13] S. Ghosh and K. V. Srivastava, "Broadband polarization-insensitive tunable frequency selective surface for wideband shielding," *IEEE Trans. Electromagn. Compat.*, vol. 60, no. 1, pp. 166–172, Feb. 2018.
- [14] R. Sivasamy, B. Moorthy, M. Kanagasabai, V. R. Samsingh, and M. G. N. Alsath, "A wideband frequency tunable FSS for electromagnetic shielding applications," *IEEE Trans. Electromagn. Compat.*, vol. 60, no. 1, pp. 280–283, Feb. 2018.
- [15] I. S. Syed, Y. Ranga, L. Matekovits, K. P. Esselle, and S. Hay, "A single-layer frequency-selective surface for ultra-wideband electromagnetic shielding," *IEEE Trans. Electromagn. Compat.*, vol. 56, no. 6, pp. 1404–1411, Dec. 2014.
- [16] *IEEE Standard for Validation of Computational Electromagnetics Computer Modeling and Simulations*, IEEE Standard 1597.1-2008, 2008.
- [17] A. P. Duffy, A. Orlandi, and G. Zhang, "Review of the feature selective validation method (FSV). Part I—Theory," *IEEE Trans. Electromagn. Compat.*, vol. 60, no. 4, pp. 814–821, Aug. 2018.
- [18] A. Orlandi, A. P. Duffy, and G. Zhang, "Review of the feature selective validation method (FSV). Part II—Performance analysis and research fronts," *IEEE Trans. Electromagn. Compat.*, vol. 60, no. 4, pp. 1029–1035, Aug. 2018.
- [19] N. Liu, X. Sheng, C. Zhang, J. Fan, and D. Guo, "A miniaturized triband frequency selective surface based on convoluted design," *IEEE Antennas Wireless Propag. Lett.*, vol. 16, pp. 2384–2387, 2017.
- [20] N. Liu, X. Sheng, C. Zhang, J. Fan, and D. Guo, "A design method for synthesizing miniaturized FSS using lumped reactive components," *IEEE Trans. Electromagn. Compat.*, vol. 60, no. 2, pp. 536–539, Apr. 2018.